JOURNAL OF THE FACULTY OF ENGINEERING, THE UNIVERSITY OF TOKYO (B)
Vol. XXXVI, No. 2 (1981)

Hysteresis Models of Reinforced Concrete for Earthquake-Response Analysis

by

Shunsuke OTANI*

(Received May 7, 1981)

Various hysteresis models for the reinforced concrete, especially simulating dominantly flexural behaviour, are described: (a) Degrading Bilinear model, (b) Ramberg-Osgood model, (c) Clough model, (d) Bilinear Takeda model, (e) Takeda model, (f) Hisada model, and (g) Degrading Trilinear model. Two types of damping are considered in the analysis; *i.e.*, (a) constant mass-proportional damping, and (b) varying instantaneous stiffness proportional damping. Hysteretic energy dissipation index is defined to quantify the fatness of a hysteresis loop.

The effect of different stiffness parameters on earthquake response of single-degree-of-freedom systems is studied. By choosing stiffness properties and hysteretic energy dissipation capacity as similar as possible, the effect of different hysteresis models on earthquake response waveforms and amplitudes is investigated.

1. Introduction

It was more than twenty years ago when the second World Conference on Earthquake Engineering was held in Tokyo in 1960. Many research papers were presented to study the elasto-plastic response of simple systems using then-developing digital computers, placing more emphasis on the development of numerical procedures for nonlinear dynamic response analysis. When numerical methods were made easily available to experimental investigators in the late 1960's, many realistic hysteresis models were developed by experimental researchers, leading a maze of hysteretic models, each claiming the best of a kind, without understanding which hysteretic properties have a significant influence on the earthquake response. The properties of a hysteresis model were studied by those who developed the model. The effect of some hysteretic characteristics on the response of single-degree-of-freedom systems was discussed by Umemura (1973) and Tani et al (1975).

This paper studies the effect of different hysteresis parameters on the earthquake response. Hysteretic models used are limited to those which simulate dominantly flexural behaviour of the reinforced concrete so as to limit the number of models.

2. Hysteretic Behaviour of Reinforced Concrete

A typical lateral load-deflection relation of the reinforced concrete is shown in Fig. 2.1. The curve was obtained from the test of a slender column (Otani and Cheung, 1981).

*Department of Architecture

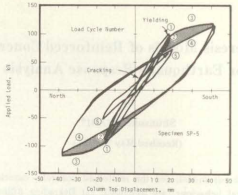

Fig. 2.1 Hysteretic behaviour of reinforced concrete

The behaviour was dominantly in flexure although the flexural cracks started to incline due to the effect of high shear before yielding. The yielding of the longitudinal reinforcement was observed in cycle 3. The general hysteretic characteristics can be summarized as follows:

(a) Stiffness changed due to the flexural cracking of concrete and the tensile yielding of the longitudinal reinforcement (cycle 1);

(b) When a deflection reversal was repeated at the same newly attained maximum amplitude, the loading stiffness in the second cycle was noticeably lower than that in the first cycle, although the resistances at the peak displacement were almost identical (cycles 3 and 4). This reduction in stiffness is attributable to the formation of cracks during loading in cycle 3, and also to a reduced stiffness of the longitudinal reinforcement in cycle 4 due to the Bauschinger effect;

(c) Average peak-to-peak stiffness of a complete cycle decreases with previous maximum displacement. Note that the peak-to-peak stiffness of cycle 5 is significantly smaller than that of cycle 2, although the displacement amplitudes of the two cycles are comparable. The peak-to-peak stiffness of cycle 5 is closer to that of cycles 3 and 4; and

(d) The hysteretic characteristics of reinforced concrete are dependent on the loading history.

A hysteretic model for the reinforced concrete must be able to represent the above characteristics. The observation is limited to a dominantly flexural behaviour of the reinforced concrete.

If the reinforced concrete is subjected to high shear stress reversals, or if the slippage of the longitudinal reinforcement within the anchorage area occurs, the force-deflection curve exhibits a pronounced pinching. The hysteretic models of such behaviour will not be discussed in this paper.

Before static force-deflection relations are used in a dynamic analysis, the effect of strain rate needs to be examined. Mahin and Bertero (1972) summarized the strain rate effect on member behaviour as follows:

(a) High strain rates increased the initial yield resistance, but caused small differences in either stiffness or resistance in subsequent cycles at the same displacement amplitudes; and

(b) Strain rate effect on resistance diminished with increased deformation in a strain-hardening range.

Note that strain rate (velocity) during an oscillation is highest at low stress levels, and that the rate gradually decreases toward a peak strain (displacement). Furthermore, damage in the reinforced concrete reduces the stiffness, elongating the period of oscillation. Therefore, the strain rate effect can be judged small on the earthquake response of a normal reinforced concrete structure. Consequently, the static hysteretic relationship can be utilized in a nonlinear dynamic analysis.

3. Hysteretic Models for Reinforced Concrete

A hysteresis model must be able to provide the stiffness and resistance under any displacement history. Many hysteresis models have been developed. Some hysteresis models are elaborate, and include many hysteretic rules. Others are simple. The complicatedness of a hystresis model indicates a larger memory to store the hysteretic rule program, but does not necessarily lead to a longer computation time because the complicatedness of a hysteretic model requires simply many branchings in a computer program, and only a few branches are referred to for a step of response computation.

Different hysteresis models representing dominantly flexural behaviour of the reinforced concrete are briefly described in this section. The following definitions are used to simplify the description of the hysteretic conditions:

loading	= the amplitude (positive or negative) of resistance increases without change in sign;
unloading	= the amplitude (positive or negative) of resistance decreases without change in sign;
load reversal	= the sign of resistance changes, and the response point crosses the displacement axis;
primary curve	= a resistance-displacement relation curve under monotonically increasing load;
unloading point	= a resistance-displacement point from which unloading has started.

The coordinates of a response point on a displacement-resistance plane are given by (D, F), in which

D = displacement
F = resistance

It is assumed that the primary curve is symmetic about its origin. The primary curve is represented by either "bilinear" or "trilinear" lines, with stiffness changes at "cracking(C)" and "yielding(Y)" points.

A hysteretic energy dissipation index (E_h) is used to express the amount of hysteretic energy dissipation ΔW per cycle during a displacement reversal of equal amplitudes in the positive and negative directions;

$$E_h = \Delta W / 2\pi F_m D_m \tag{3.1}$$

in which F_m is the resistance at the peak displacement D_m (Fig. 3.1). The value of the index is equal to the equivalent viscous damping factor of a linearly elastic system which is capable of dissipating energy ΔW in one cycle under the "resonant steady-state" oscillation.

Bilinear Hysteresis Model: At the initial development stage of nonlinear dynamic analysis, the elastic-perfectly plastic hysteretic model (elasto-plastic model) was used by many investigators. A finite positive slope was assigned to the stiffness after yielding to simulate the strain hardening characteristics of the steel and the reinforced concrete (Bilinear model).

When the degradation in stiffness was recognized in the behaviour of the reinforced concrete, the loading and unloading stiffness K_r was proposed to decrease with the previous maximum displacement (Nielsen and Imbeault, 1970) in a form:

$$K_r = K_y \left| \frac{D_m}{D_y} \right|^{-\alpha} \tag{3.2}$$

in which,

α = unloading stiffness degradation parameter ($0 \leqq \alpha \leqq 1.0$);
K_y = initial elastic stiffness; and
D_m = previously attained maximum displacement in any direction.

The unloading stiffness remains constant until the response displacement amplitude

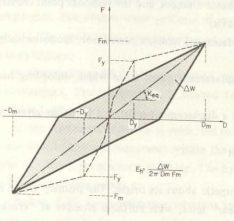

Fig. 3.1 Hysteretic energy dissipation index

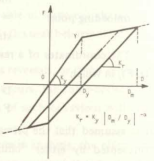

Fig. 3.2 Degrading bilinear hysteresis model

exceeds the previous maximum displacement in either direction. The model is called a "(degrading) bilinear" hysteresis model (Fig. 3.2). If the value of α is chosen to be zero, the unloading stiffness does not degrade with yielding. Normally, a value of constant α is suggested between 0.1 and 0.5 for the reinforced concrete. A smaller value of α tends to yield a larger residual displacement. The degrading bilinear model does not dissipate hysteretic energy until the yielding is developed.

The hysteretic energy dissipation index of the degrading bilinear model is given by

$$E_h = \frac{2(1-\beta)\{\mu - \mu^{\alpha}(1-\beta+\mu\beta)\}}{\pi\mu(1-\beta+\mu\beta)(1-\beta\mu^{\alpha})} \tag{3.3}$$

in which

β = ratio of post-yielding stiffness to initial elastic stiffness; and
μ = ductility factor (ratio of maximum displacement to the initial yield displacement).

The equation is valid only when a ductility factor is greater than unity. Figure 3.3 shows the relationship between the hysteretic energy dissipation index and the ductility factor for $\beta = 0.10$. The index increases rapidly when the ductility factor increases from 1.0 to 2.0, and peaks when the ductility factor ranges from 4.0 to 6.0. For a given ductility factor, the index increases with the decrease of the unloading stiffness degradation parameter. The hysteretic energy dissipation index of a regular bilinear model ($\alpha=0$) reaches as high as 0.33 at a ductility factor of 4.0.

Ramberg-Osgood Model: A stress-strain relation of metal was expressed by Ramberg and Osgood (1943). Jennings (1963) introduced the fourth parameter to the model.

The initial loading curve of the model as modified by Jennings is expressed by

$$\frac{D}{D_y} = \frac{F}{F_y}\left(1 + \eta \left| \frac{F}{F_y} \right|^{\gamma-1}\right) \tag{3.4}$$

in which

γ = exponent of Ramberg-Osgood model; and
η = parameter introduced by Jennings.

The initial tangent modulus is equal to (F_y/D_y), and the initial loading curve passes a point $(F_y, (1+\eta)D_y)$ for any value of γ as demonstrated in Fig. 3.4. The shape of the primary curve can be controlled by the exponent γ from linearly elastic ($\gamma=1.0$) to elasto-plastic ($\gamma=\infty$). For a larger value of γ, the behaviour becomes similar to that of the bilinear model. Upon unloading from a peak response point (D_0, F_0), the unloading, load reversal and reloading branch of the relationship (Fig. 3.5) is given by

$$\frac{D-D_0}{2D_y} = \frac{F-F_0}{2F_y}\left(1 + \eta \left| \frac{F-F_0}{2F_y} \right|^{\gamma-1}\right) \tag{3.5}$$

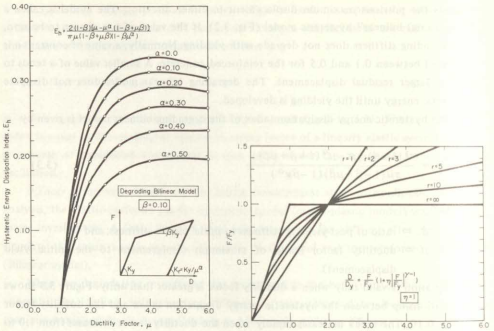

Fig. 3.3 Hysteretic energy dissipation index of degrading bilinear model ($\beta = 0.10$)

Fig. 3.4 Ramberg-Osgood function

until the response point reaches the peak point of one outer hysteresis loop.

The resistance at a given displacement can be computed by solving either Eq. 3.4 or Eq. 3.5 by the Newton-Rapson's iterative procedure.

The hysteretic energy dissipation index of the Ramberg-Osgood model is expressed as

$$E_h = \frac{2}{\pi}\left(1 - \frac{2\eta}{\gamma+1}\right)\left(1 - \frac{D_y}{F_y}\frac{F_m}{D_m}\right) \tag{3.6}$$

and is shown in Fig. 3.6 when the parameter η is unity. The model can dissipate some hysteretic energy even if the ductility factor is less than unity. The index is sensitive to the exponent γ of the model, and the hysteretic energy dissipation capacity increases with increasing value of the exponent.

Clough Degrading Stiffness Model: A hysteretic model with a trilinear primary cruve was proposed by Hisada, Nakagawa and Izumi (1962) to represent the hysteretic behaviour of a reinforced concrete structure (Hisada Model). The unloading stiffness is kept equal to the initial elastic stiffness despite of structural damage. On the other hand, the response point moves toward a maximum response point in the direction of loading, simulating the stiffness degradation with deformation.

A similar model, with a bilinear primary curve, was proposed by Clough and Johnston (1966), called the Clough model.

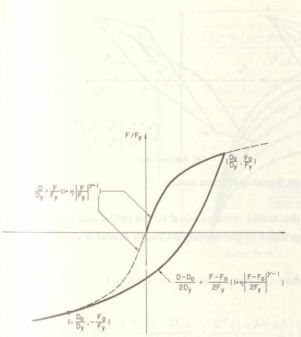

Fig. 3.5 Hysteretic relation of Ramberg-Osgood model

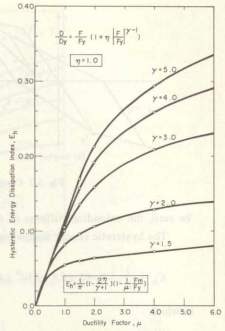

Fig. 3.6 Hysteretic energy dissipation index of Ramberg-Osgood model

A minor deficiency of the Clough model was pointed out by Mahin and Bertero (1976). In Fig. 3.7.a, after unloading from point A, consider a situation in which reloading takes place from point B. The original Clouth model assumed that the response point should move toward the previous maximum response point C. This is not realistic. Therefore, a minor modification was added so that the response point should move toward an immediately preceding unloading point A during reloading. When the response point reaches the point A, the response point moves toward the previous maximum point C (Fig. 3.7.b).

The model was made more versatile in this paper by incorporating the reduction in unloading stiffness K_r with a maximum displacement in a form:

$$K_r = K_y \left|\frac{D_m}{D_y}\right|^{-\alpha} \tag{3.7}$$

in which,

α = unloading stiffness degradation parameter;
K_y = initial elastic stiffness; and
D_m = previous maximum displacement

Note that unloading stiffness in the positive and negative resistance regions are not the same in this modified Clough model (Fig. 3.7.b) because the unloading stiffness degrades with the maximum displacement attained in the direction. If the value of α is chosen to

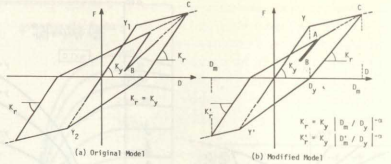

Fig. 3.7 Clough degrading stiffness models

be zero, the unloading stiffness of the model remains equal to the initial elastic stiffness.

The hysteretic energy dissipation index of the modified Clough model is given by

$$E_h = \frac{1}{\pi}\left\{1-(1-\beta+\mu\beta)\mu^{\alpha}/\mu\right\} \tag{3.8}$$

in which

β = ratio of post-yielding stiffness to initial elastic stiffness; and
μ = ductility factor (maximum displacement divided by yield displacement).

The equation is valid for a ductility factor larger than unity. The hysteretic energy dissipation index and ductility relations are given in Fig. 3.8 for different values of unloading stiffness degradation parameter. The Clough model can continuously dissipate hystertic energy even at a small amplitude oscillation after yielding.

Takeda Model: Based on the experimental observation on the behaviour of a number of medium-size reinforced concrete members tested under lateral load reversals with light to medium amount of axial load, a hysteresis model was developed by Takeda, Sozen and Nielsen (1970). Takeda's model included (a) stiffness changes at flexural cracking and yielding, (b) hysteresis rules for inner hysteresis loops inside the outer loop, and (c) unloading stiffness degradation with deformation. The response point moves toward a peak of the one outer hystersis loop. The unloading stiffness K_r is given by

$$K_r = \frac{F_c+F_y}{D_c+D_y}\left|\frac{D_m}{D_y}\right|^{-\alpha} \tag{3.9}$$

in which

α = unloading stiffness degradation parameter; and
D_m = previous maximum displacement in the direction concerned.

The hysteresis rules are extensive and thorough (Fig. 3.9).

The hysteretic energy dissipation index of the Takeda model is expressed as

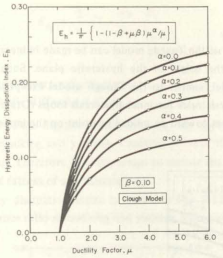

Fig. 3.8 Hysteretic energy dissipation index of Clough model (β = 0.10)

$$E_h = \frac{1}{\pi}\left\{1-\frac{1+(D_c/D_y)}{1+(F_c/F_y)}\cdot\frac{\mu^{\alpha}(1-\beta+\mu\beta)}{\mu}\right\} \tag{3.10}$$

The expression is valid for a ductility factor greater than unity. The relationship between the hysteretic energy dissipation index and ductility is shown in Fig. 3.10 when the post-yielding stiffness is 10% of the yielding stiffness ($K_y = F_y/D_y$). The general trend is similar to the one for the Clough model, although the index is positive when the

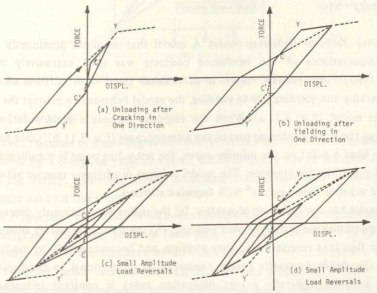

Fig. 3.9 Takeda hysteresis model

ductility factor is unity.

The primary curve of the Takeda model can be made bilinear simply by choosing the cracking point to be the origin of the hysteretic plane. Such a model is called the "bilinear Takeda" model, similar to the Clough model except that the bilinear Takeda model has more hysteresis rules for inner hysteresis loops (Otani and Sozen, 1972); *i.e.*, the response point moves toward an unloading point on the immediately outer hysteresis loop.

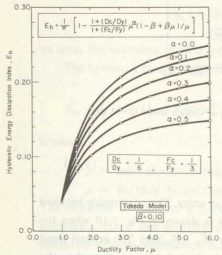

Fig. 3.10 Hysteretic energy dissipation index of Takeda model ($\beta = 0.10$)

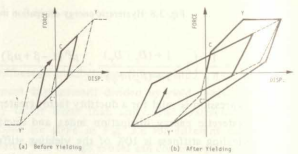

Fig. 3.11 Degrading trilinear model

Degrading Trilinear Hysteresis Model: A model that simulates dominantly flexural stiffness characteristics of the reinforced concrete was used extensively in Japan (Fukada, 1969). The primary curve is of trilinear shape with stiffness changes at flexural cracking and yielding. Up to yielding, the model behaves in a manner the same as the bilinear model (Fig. 3.11.a). When the response exceeds a yield point, response point follows the strain-hardening part of the primary curve (Fig. 3.11.b). Once unloading takes place from a point on the primary curve, the unloading point is considered to be a new "yield point" in the direction. The model behaves in a bilinear manner between the positive and negative "yield points" with degraded stiffness.

This model has the following properties: (a) the stiffness continuously degrades with increasing maximum amplitude beyond yielding, (b) the hysteretic energy dissipation is large in the first load reversal cycle after yielding, and becomes steady in the following cycles, (c) the steady hysteretic energy dissipation is proportional to the displacement amplitude, and the hysteretic energy dissipation index is constant independent of displacement and post-yield stiffness.

The hysteretic energy dissipation index of a degrading trilinear model is given by

$$E_h = \frac{2}{\pi}\left(1 - \frac{K_y}{K_c}\right)\frac{F_c}{F_y} \tag{3.11}$$

in which

K_y = yielding stiffness ($= F_y/D_y$); and
K_c = initial elastic stiffness ($= F_c/D_c$).

The index is independent of the displacement amplitude, but dependent on the stiffness and resistance ratioes at cracking and yielding. Cracking point of this model controls the fatness of a hysteresis loop. Therefore, it is important to choose the cracking point taking into account the degree of fatness of a hysteresis loop.

The hysteretic energy dissipation index is shown in Fig. 3.12. The index increases proportional to the resistance ratio at cracking and yielding for a given stiffness ratio.

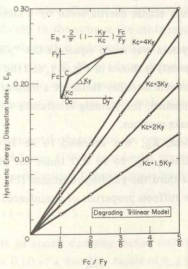

Fig. 3.12 Hysteretic energy dissipation index of degrading trilinear model

4. Method of Analysis

Nonlinear response of single-degree-of-freedom (SDF) systems to earth-quake motion was computed by a computer program (SDF), which currently has 14 different hysteresis models in the library. Hysteresis models simulating flexural behaviour of the reinforced concrete were used for this study.

Model Properties: The effect of different hysteresis model on earthquake response is to be investigated. Therefore, common force-deflection properties should be specified to all the models so that the influence of different model hysteretic behaviour would be clarified. However, some models (Takeda, Hisada, and Degrading Trilinear models) have a trilinear primary curve under monotonically increasing load, and others (Bilinear, Clough, and Bilinear Takeda models) have a bilineary primary curve. Consequently, the

yield point and the post-yielding stiffness were chosen common among the models, and the cracking point was added to the models with a trilinear primary curve.

The mass of an SDF system was arbitrarily chosen to be 1.00 ton since the overturning effect due to the mass' side sway was not included in the analysis. A series of hysteretic models were designed with "yield periods" (periods related to the secant stiffness at the yield point) of 0.10, 0.14, 0.20, 0.28, 0.40, 0.57, 0.80, 1.13, and 1.60 sec.

Earthquake response amplitudes are known to vary with the system's period and the yield level. To make the comparative study easy, SDF systems with different periods were desired to produce comparable ductility ratioes (attained maximum displacement divided by the yield value). Hence, the Newmark's design criterai (Veletsos and Newmark, 1960) were adopted. Namely, the yield resistance of an SDF system was determined by:

(a) dividing the maximum elastic enertia force by the allowable ductility factor, μ, of the system if the system's period is greater than 0.5 sec; and

(b) dividing the maximum elastic enertia force by a factor $\sqrt{2\mu-1}$ if the system's period less than 0.5 sec.

The stiffness of an elastic system was made equal to the "yielding stiffness", K_y (the secant stiffness at the yield point) as shown in Fig. 4.1, and the damping factor was 5 per cent of the critical. The allowable ductility factor of a nonlinear system was arbitrarily assumed to be 4.0. In this manner, the yielding resistances were different for different periods and different earthquake motions.

The post-yielding stiffness, K_u, was assumed to be 10 percent of the yielding stiffness; the uncracked stiffness, K_c, to be 2.0 times the yielding stiffness; and the cracking resistance to be one-third the yielding resistance (Fig. 4.1). These assumptions were used to approximate the stiffness properties of a reinforced concrete structure.

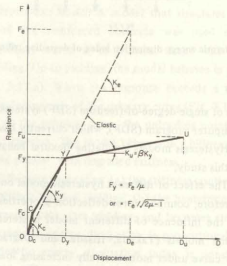

Fig. 4.1 Determination of stiffness properties

Table 4.1 Hysteretic energy dissipation index
(Ductibity factor = 4)

Model	Hysteretic Energy Dissipation Index
Clough Model (α = 0.5)	0.11
Degrading Trilinear Model	0.11
Takeda Model (α = 0.5)	0.14
Bilinear Model (α = 0.5)	0.19
Clough Model (α = 0.0)	0.21
Takeda Model (α = 0.0)	0.23
Ramberg-Osgood Model	0.28
Bilinear Model (α = 0.0)	0.33

α = Unloading stiffness degradation parameter

The parameters of the Ramberg-Osgood model were chosen so that the resistance at the allowable ductility should be the same as the other models; *i.e.*, $\eta = 1.0$ and $\gamma = 3.79$.

The hysteretic energy dissipation index of different models is listed in *Table 4.1*. The ductility factor is assumed to be 4.0. Note a large descrepancy among the models in the capacity to dissipate hysteretic energy under a steady-state condition. The unloading stiffness degradation parameter α has an appreciable effect on the value of hysteretic energy dissipation index.

On the basis of experimental observation on one-story one-bay reinforced concrete frame models, Gulkan and Sozen (1974) proposed a simple expression for a "substitute damping factor" for use in equivalent linear response analysis. The expression is given as;

$$h_{eq} = 0.02 + 0.2\,(1 - 1/\sqrt{\mu}) \tag{4.1}$$

The first term represents an elastic damping factor, and the second term the hysteretic energy loss, which yields 0.10 at a ductility factor of 4, a value comparable to hysteretic energy dissipation indices for the Clough, Bilinear Takeda and Takeda models with α = 0.5.

Damping: Viscous damping was assumed in this study. The damping coefficient was assumed to be made of two parts: one part proportional to the constant mass, and the other proportional to the varying instantaneous stiffness;

$$C = C_m M + C_k K^* \tag{4.2}$$

in which

C = damping coefficient;

M = mass ; and

K^* = instantaneous stiffness.

If an instantaneous apparent damping factor h_{app} is defined in the following form,

$$h_{app} = C / 2\sqrt{MK^*} \tag{4.3}$$

Then, the apparent damping factor is expressed as

$$h_{app} = \frac{C_m}{2} \frac{M}{\sqrt{K^*}} + \frac{C_k}{2} \frac{K^*}{\sqrt{M}} \tag{4.4}$$

As the stiffness degrades with damage, the apparent damping factor related to the mass is expected to increase and that related to the instantaneous stiffness tends to decrease.

Earthquake Records: Four earthquake accelerograms from two California earthquakes were used in this study: the NS and EW components of the 1940 El Centro record and the N21E and S69E components of the 1952 Taft record (Fig. 4.2), digitized at the University of Illinois at Urbana-Champaign (Amin and Ang, 1966). Linearly elastic response spectra of these four records were studied using the entire duration and the first 15-sec. portion of the records. The damped spectra were almost identical for a period range less than 2.0 sec. using either the entire duration or the first 15-sec. portion except for the El Centro (EW) record. Consequently, the response computation was terminated approximately at 15 sec. when the Taft (N21E), Taft (S69E), and El Centro (NS) records were used in the current study. On the other hand, the maximum response of some linearly elastic systems under the El Centro (EW) motion occurred after 15 sec.

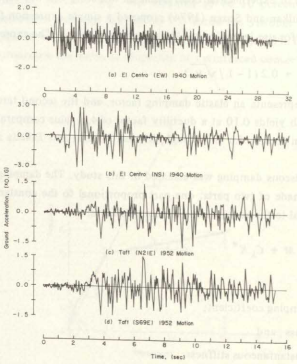

Fig. 4.2 Earthquake accelerograms

Therefore, the entire 30-sec. record of the El Centro (EW) motion was used. The response spectra of the four records are shown in Fig. 4.3.

Numerical Method: The equation of motion was solved numerically using the Newmark-β method (Newmark, 1959) with $\beta = 1/6$ and $\gamma = 1/2$. Both the equation of motion and the displacement-velocity-acceleration relations were satisfied only at the discrete time step using an iterative procedure. In other words, the "overshooting" of the hysteresis curve was adjusted within the time step.

A constant time increment of the numerical integration was taken either as one-twentieth the initial elastic period or 0.02 sec., whichever was shorter. The former

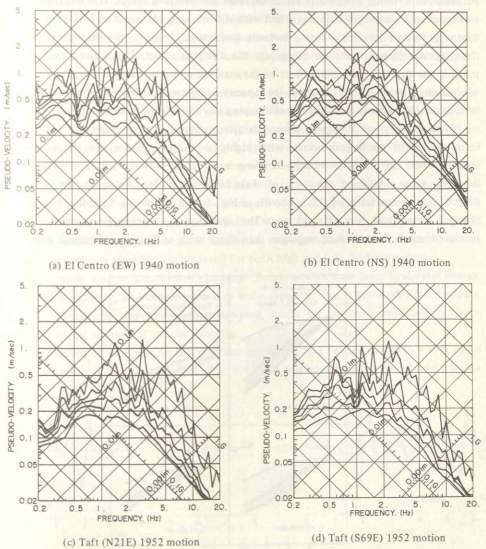

(a) El Centro (EW) 1940 motion

(b) El Centro (NS) 1940 motion

(c) Taft (N21E) 1952 motion

(d) Taft (S69E) 1952 motion

Fig. 4.3 Response spectra of earthquake records
(Damping factors = 0.00, 0.02, 0.05, 0.10, 0.20)

was necessary to faithfully trace the hysteresis curve rather than the numerical stability requirements. The latter criterion became necessary because the earthquake accelerograms were given at a 0.02-sec. interval.

5. Effect of Damping

Two types of viscous damping were considered in this study; *i.e.*, (a) damping coefficient proportional to the constant mass, and (b) damping coefficient proportional to the varying instantaneous stiffness. The constant mass-proportional damping tends to yield an increasing apparent damping factor with the degradation of stiffness, whereas the varying stiffness-proportional damping tends to decrease the damping effect. It is not reasonable to expect such increasing damping effect with stiffness degradation if an SDF system also dissipates hysteretic energy during inelastic oscillation. However, the mass-proportional damping was found useful to exaggerate the damping effect. For a given earthquake motion, the degree of damping effect on the maximum response may depend on (a) type of damping, (b) period of vibration, (c) capacity of hysteretic energy dissipation, and (d) level of ductility demand. The effect of damping is studied from these viewpoints.

Type of Damping: Mass-proportional damping is expected to be more effective where many cycles of oscillation occurs with highly degraded stiffness. On the contrary, instantaneous stiffness-proportional damping is effective during oscillation in a small ductility range. Attained ductility of Takeda models with an unloading stiffness degradation parameter α of 0.0 is shown in Fig. 5.1, in which the "yielding period" is changed from 0.14 sec. to 1.13 sec. The system with mass-proportional damping produced small displacement response than those with stiffness-proportional damping

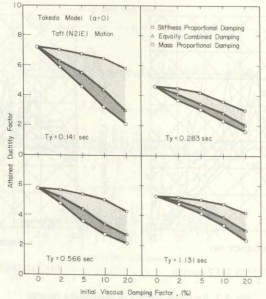

Fig. 5.1 Effect of mass-proportional and stiffness-proportional damping

having the same initial damping factor. With an increase in the value of initial damping factor, the mass-proportional damping is more effective in reducing the response amplitude. This tendency is larger for a shorter period system. The response amplitudes of systems with stiffness-proportional damping are not so sensitive to the increase in the value of initial damping factor partially attributable to the fact that the hysteretic energy dissipation is appreciable when the unloading stiffness degradation parameter α was 0.0. When the initial damping factor is made of equal contributions of mass-proportional and stiffness-proportional dampings, the mass-proportional damping tends to have a dominant influence on the maximum response.

Displacement response waveforms are compared in *Fig. 5.2*, for two types of damping. The waveforms are generally similar. The effect of damping type is cospicuous when an unloading stiffness degradation parameter α is 0.5; *i.e.*, the hysteretic energy dissipation is small. The systems with stiffness-proportional damping produce a larger response.

Period and Ductility Range: The effect of mass-proportional damping on maximum response is pronounce, and the mass-proportional damping was found useful to exaggerate the damping effect and clarify a general trend of the damping effect on maximum response. Therefore, the mass-proportional damping is used here. Figure 5.3 shows the variation of maximum response with the amout of damping. The maximum response is reduced significantly with increasing damping amplitude in short-period systems (T_y = 0.14 sec), but is not so much affected in long-period systems (T_y = 1.13 sec). The yield resistance level was varied to study the effect of damping at different ductility ranges. the general trend of decreasing response amplitude with logarithmically increasing damping amplitude is observed for both high and low ductility ranges.

Hysteretic Energy Dissipation Capacity: Some models have large hysteretic energy dissipation capacity, and others have very little capacity. The latter model can dissipate kinetic energy only through viscous damping, hence its response amplitude is likely affected by the amount of viscous damping.

The effect of damping on the response amplitude of a Takeda model (α = 0.0) and a Peak-Oriented model is studied in Fig. 5.4. The response point of the Peak-Oriented

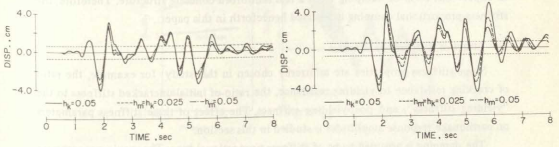

(a) Takeda Model (α = 0.0) (b) Takeda Model (α = 0.5)

Fig. 5.2 Effect of Damping Type on Response Waveforms – El Centro (NS) 1940 Motion, T_Y = 0.40 sec. –

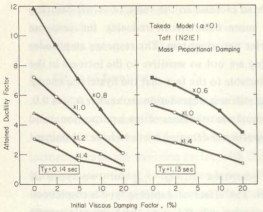

Fig. 5.3 Effect of damping with ductility and period

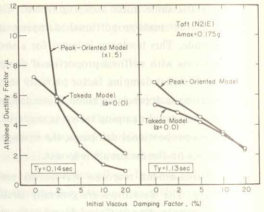

Fig. 5.4 Effect of damping with hysteretic energy dissipation capacity

hysteresis model moves toward a maximum response point in the loading direction, and the model behaviour is linearly elastic between the positive and negative maximum response points without any hysteretic energy dissipation. Once the response point reaches a maximum response point, it moves on the primary curve. The maximum response of the Peak-Oriented model at a yielding period of 0.14 sec. was too large, and the yield resistance was increased by 50 per cent from the standard value to reduce the response amplitude.

Note that the amount of damping has a larger influence on the response ductility of Peak-Oriented models, especially in a short period range. The difference in ductility of the two models was relatively small in a long-period range.

Summary Mass-proportional damping is effective in reducing the response of nonlinear system, especially in a short period range. Stiffness-proportional damping has much less effect on the maximum response, especially when the model is capable of dissipating a large hysteretic energy. The effect of viscous damping is larger on maximum response of a system with a smaller hysteretic energy dissipation capacity.

Although the mass-proportional damping was used in this section, it is not probable to expect this form of damping from a real reinforced concrete structure. Therefore, the stiffness-proportional damping is assumed henceforth in this paper.

6. Effect of Stiffness Parameters

Some stiffness properties are arbitrarily chosen in this study: for example, the ratio of cracking resistance to yielding resistance, the ratio of initial uncracked stiffness to the "yielding stiffness", and post-yielding stiffness. The effect of these stiffness parameters on earthquake response amplitudes is studied in this section.

The damping is assumed to be of stiffness-proportional type. The maximum response of an SDF system is not so sensitive to the amplitude of initial damping factor. Therefore, an initial elastic damping factor of 0.05 is used for a system with bilinear primary curve,

and 0.0707 for a system with trilinear primary curve. In this manner, the damping factor of all the systems is made identical at the yielding period because the pre-cracking stiffness of a trilinear primary curve is chosen twice the yielding stiffness.

Unloading Stiffness Degradation Parameter: Some models use an unloading stiffness degradation parameter, which controls the fatness of a hysteresis loop and also the plastic residual deformation. It is not possible to determine the value of this parameter from the material and geometrical properties of a reinforced concrete structure. Normal range of this parameter is 0.0 to 0.5, and a value of 0.4 has been often used for the reinforced concrete.

The effect of the value of the unloading stiffness degradation parameter on maximum response of Takeda models is shown in Fig. 6.1.a. Maximum response increases with an increasing value of the parameter, and this tendency is remarkable for shorter period systems. As already seen in the study on damping effect, the system's capacity (either through damping or through hysteresis) to dissipate kinetic energy has a conspicuous influence on the maximum response of a short period structure. The same tendency is observed in Fig. 6.1.b. when the yielding period of systems was varied from 0.1 to 1.60 sec.

Response waveforms of Takeda models under El Centro (NS) 1940 motion are compared in Fig. 6.2.a. The yielding period of the systems is 0.4 sec. The yield level was chosen to be 0.6 times that of the standard model. For a large value of the parameter, peak amplitudes are larger both in the positive and negative directions, having comparable amplitudes in the two directions. For smaller values of the parameter, the system tends to produce large amplitudes only in one direction. This is clearly observed in the hysteretic curve shown in Fig. 6.2.c. Peak-to-peak stiffness in a low amplitude oscillation is lower

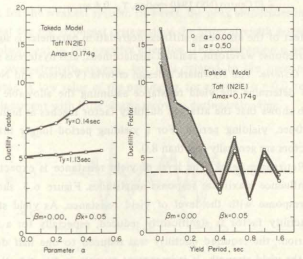

(a) Unloading stiffness degradation parameter

(b) Design criteria

Fig. 6.1 Maximum response with unloading stiffness degradation parameter and yielding period

for a system with a larger parameter, causing a longer period of oscillation from approximately 6.0-sec. in Fig. 6.2.a.

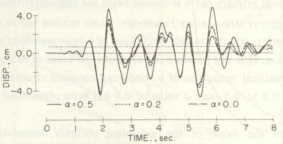

(a) Response waveforms

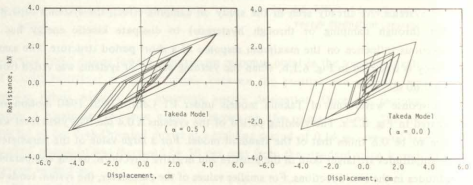

(b) Hysteresis (α = 0.5) (c) Hysteresis (α = 0.0)

Fig. 6.2 Response waveforms and unloading stiffness degradation parameters – El Centro (NS) 1940 motion, T_y 0.4 sec. –

The effect of the unloading stiffness degradation parameter is significant on response amplitude, response waveform, residual displacement, and hysteresis shape.

Design Criteria: The Newmark's design criteria (Veletsos and Newmark, 1960) were adopted to determine the yield resistance assuming the allowable ductility to be 4.0. Figure 6.1.b shows that the attained ductility factor reaches as high as 17.1 for a system with a 0.10-sec. yielding period. For a yielding period longer than 0.2 sec., attained ductility factors are generally less than 8.0.

Yield Resistance Level: The level of yield resistance is expected to be one major factor to influence maximum response amplitudes. Figure 6.3 shows the variation of maximum response with the level of yield resistance. As yield strength increases, an attained ductility factor is significantly reduced, especially for a system with a short yielding period: the required ductility was reduced to one half due to a 30 per cent increase in the yield strength. It is important to note in Fig. 6.3 that the value of yield displacement increased proportional to the level of yield resistance. Consequently the maximum response amplitude did not decrease with the level of yield resistance so much

as the attained ductility did, although the 0.14-sec. period system showed a rapid increase in the displacement amplitude with the reduction in yield strength. The 1.13-sec. system also showed an increase in maximum displacement with decreasing yield strength, but reached a peak at the standard yield resistance, and then gradually decreased its maximum displacement amplitude.

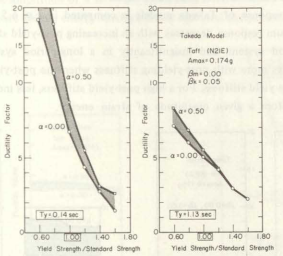

Fig. 6.3 Maximum response with yield resistance level

Response waveforms of Takeda models (α = 0.0) with different yield resistances are compared in Fig. 6.4. The yield resistances are 0.70, 0.60, 0.47 times the standard yield strength at a 0.4-sec. yield period under El Centro (NS) 1940 motion. The maximum amplitude is largest for the weakest system. However, the peak amplitudes in the positive direction were largest for the strongest system since the lower strength systems produced a large residual displacement in the negative direction. This observation is not necessarily true for a general weak-strength system, but it is related to the unloading stiffness degradation parameter. A low value of the parameter, for example α = 0.0, tends to cause a large residual displacement with little elastic recovery during unloading.

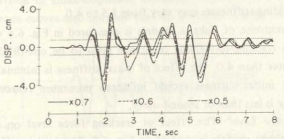

Fig. 6.4 Response waveforms with different yield resistance – El Centro (NS) 1940, T_y = 0.40 sec. –

The level of yield resistance has a significant effect on maximum response amplitude, especially in a short-period range.

Post-Yielding Stiffness: The strain hardening of reinforcing bars will give a finite positive stiffness even after the flexural yielding. Very smal post-yielding stiffness has been routinely used in Japan. The standard model in this paper assumes a 10 per cent of the yielding stiffness as the post-yielding stiffness.

Maximum response of Takeda models is compared in Fig. 6.5 varying post-yield stiffness. Maximum response decreases with an increasing post-yield stiffness, remarkably in a short-period system, and insignificantly in a long-period system. The response amplitude changes more with post-yielding stiffness when the post-yield stiffness is 0.05 to 0.20 times the yield stiffness. For a high post-yield stiffness, less inelastic displacement is required to store a given magnitude of strain energy.

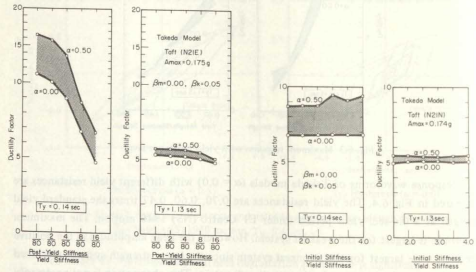

Fig. 6.5 Maximum response with post-yield stiffness

Fig. 6.6 Maximum response with initial stiffness

Initial Stiffness: The initial stiffness was arbitrarily chosen in this paper to be 2.0 times the yielding stiffness. For a normal reinforced concrete member, the ratio of initial to the yielding stiffnesses may vary from 1.5 to 4.0.

Maximum response of Takeda models is compared in Fig. 6.6 varying the stiffness ratio, keeping a cracking-to-yielding resistance ratio to be one-third. When an attained ductility is greater than 4.0, the effect of initial stiffness is minimal. It is naturally expected that the initial stiffness should influence maximum response amplitude if an attained ductility is less than or around unity.

Cracking Force Level: The effect of cracking force level on maximum response amplitude of Takeda models is studied in Fig. 6.7. The initial stiffness was kept to be 2.0 times the yielding stiffness. Little effect is observed when an attained ductility is greater than 4.0 even in a short-period system.

The hysteretic energy dissipating capacity of a Degrading Trilinear model is known to be sensitive to the choice of a cracking point relative to the yielding point. The effect of cracking force level on maximum response amplitude of Degrading Trilinear models is studied in Fig. 6.8. An attained ductility factor decreases with an increasing cracking force level, especially in a short-period system. This is another example to show that maximum response amplitude of a short-period system is significantly influenced by the capability to dissipate kinetic energy through either damping or hysteresis.

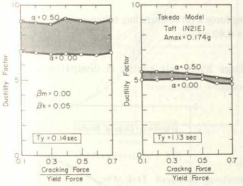

Fig. 6.7 Maximum response with cracking force level – Takeda model –

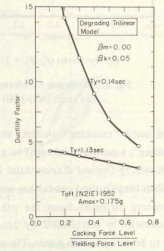

Fig. 6.8 Maximum response with cracking force level – degrading trilinear model–

Response waveforms of Degrading Trilinear models are compared in Fig. 6.9.a varying the cracking force level. The two systems oscillate almost equally in the positive and negative directions. A system with a cracking-to-yielding force ratio of one-third oscillates with larger amplitudes. The response waveforms are in phase up to 6.0 sec. from the beginning, and then a low-cracking-force system starts to oscillate in a longer period. By comparing hysteresis shapes of the two systems in Fig. 6.9.b and c, it can be seen that a peak-to-peak stiffness of small-amplitude oscillation is lower for a low-cracking force system. The hysteresis curves also indicate that no hysteresis energy is dissipated by the

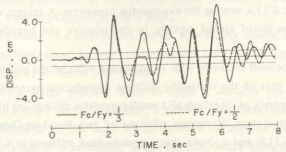

(a) Response waveforms

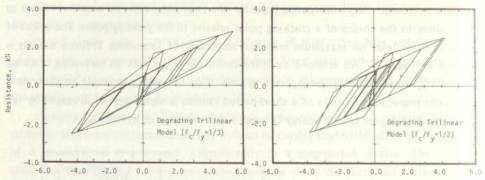

(b) Hysteresis (F_c/F_y = 1/3) (c) Hysteresis (F_c/F_y = 1/2)

Fig. 6.9 Response waveforms and cracking force level of degrading trilinear model – El Centro (NS) 1940 motion, T_y = 0.40 sec. –

model until "cracking" occurs, and that a large hysteresis energy is dissipated upon "cracking", a property inherent to a bilinear model.

Ramberg-Osgood Exponential Parameter: The Ramberg-Osgood model has stiffness parameters different from the other models. A parameter η introduced by Jennings (1963) is set to be unity in this paper. The effect of an exponent γ on maximum response is studied in Fig. 6.10. A Ramberg-Osgood model becomes similar to a regular Bilinear model when the exponential parameter increases. A smaller value of the parameter makes the post-yield stiffness steeper. A short-period system has a tendency to increase its maximum response with an increasing value of the parameter, whereas a long-period system slightly decreases its response.

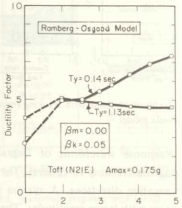

Fig. 6.10 Maximum response with Ramberg-Osgood exponential parameter

Response waveforms of Ramberg-Osgood models under El Centro (NS) 1940 motion are compared in Fig. 6.11.a varying the exponential parameter. A system with a low value of the parameter oscillated almost equally in the positive and negative directions at large amplitudes.

Residual displacement increases with an increasing value of the parameter, the effect which is similar to that of the unloading stiffness degradation parameter of a Takeda model. Dominant periods of vibration of a small-parameter system are longer than those of a large-parameter system. Hysteresis relations of two Ramberg-Osgood models are compared in Fig. 6.11.b and c. Note that a peak-to-peak stiffness at a small-amplitude

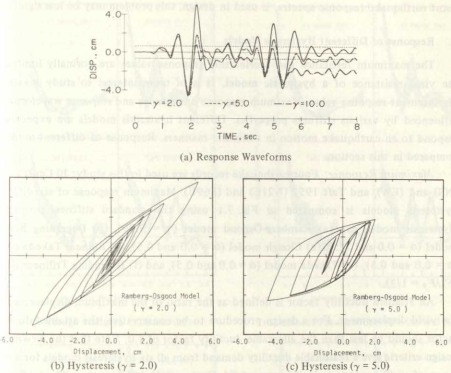

(a) Response Waveforms

(b) Hysteresis (γ = 2.0) (c) Hysteresis (γ = 5.0)

Fig. 6.11 Response waveforms and Ramberg-Osgood parameter – El Centro (NS) 1940 motion, T_y = 0.40 sec. –

oscillation is lower for a larger-parameter system.

Summary: Maximum response amplitude of a short-period system (for example, yielding period less than 0.2 sec.) increases remarkably when the system has a low capability to dissipate kinetic energy through hysteresis; *i.e.*, the unloading stiffness degradation parameter and post-yielding stiffness of the Takeda model, or cracking force level of the Degrading Trilinear model has a significant influence on the maximum response amplitude of a short-period system.

When the unloading stiffness is larger, its displacement response waveform tends to exhibit a larger residual displacement. This tendency is observed when the unloading stiffness degradation parameter of the Takeda model is small or when the exponential parameter of the Ramberg-Osgood model is large.

Response amplitude of a long-period system is relatively insensitive to the variation of stiffness parameters except for the yield resistance level, which has a dominant effect on attained ductility of nonlinear SDF systems.

The Newmark's design method tends to cause a ductility much larger than the allowable value in a short period range (say, a yielding period less than 0.3 sec). However, this may be attributable to the usage of an idividual earthquake response spectrum in designing SDF systems. If a smoothed design spectra, which gives the upper bound to

most earthquake response spectra, is used in design, this problem may be less significant.

7. Response of Different Hysteresis Models

The maximum resistance and acceleration response values are normally limited by the yield resistance of a hysteretic model. It is of more interest to study maximum displacement response value. Maximum response amplitudes and response waveforms are influenced by various stiffness properties. Different hysteresis models are expected to respond to an earthquake motion in dissimilar manners. Response of different models is compared in this section.

Maximum Response: Four earthquake records are used in this study: El Centro 1940 (NS) and (EW), and Taft 1952 (N21E) and (S69E). Maximum response of six different hysteresis models is compared in Fig. 7.1 using the standard stiffness properties. Hysteresis models are (a) Ramberg-Osgood model (γ = 3.79), (b) Degrading Bilinear model (α = 0.0 and 0.5), (c) Clough model (α = 0.0 and 0.5), (d) Bilinear Takeda model (α = 0.0 and 0.5), (e) Takeda model (α = 0.0 and 0.5), and (f) Degrading Trilinear model (F_c/F_y = 1/3).

An attained ductility factor is defined as the ratio of the maximum displacement to the yield displacement. For a design procedure to be conservative, the attained ductility factor should be less than the allowable ductility factor of 4.0. Note that the Newmark's design criteria give a reasonable ductility demand from all six hysteresis models for a wide range of yielding periods in the case of El Centro (NS) 1940 motion. The undamped yield period is a period associated with a secant stiffness at the yield point. The initial

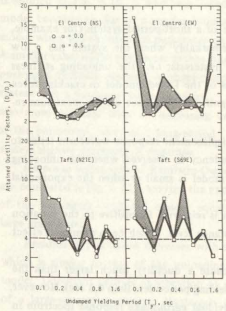

(a) Degrading bilinear model (α = 0.0 and 0.5)

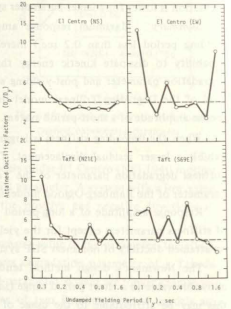

(b) Ramberg-Osgood model (γ = 3.79)

Fig. 7.1 Maximum response to different earthquake motions

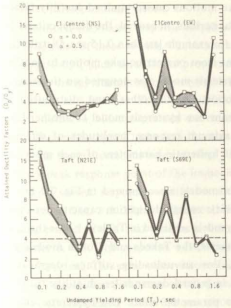

(c) Clough model (α = 0.0 and 0.5)

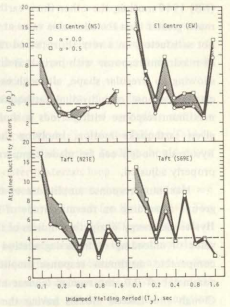

(d) Bilinear Takeda model (α = 0.0 and 0.5)

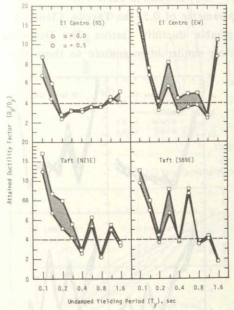

(e) Takeda model (α = 0.0 and 0.5)

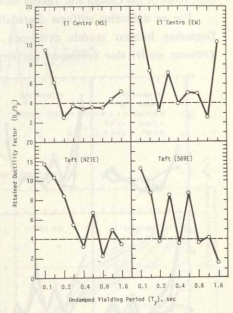

(f) Degrading trilinear model (F_c/F_y = 1/3)

Fig. 7.1 (Cont'd) Maximum response to different earthquake motions

uncracked period of an SDF system with a trilinear primary curve is approximately 70 per cent of the yield period.

Although the Newmark's design criteria appear to be acceptable for the El Centro

(NS) 1940 motion, the other three earthquake motions caused attained ductility factors much greater than the allowable value at various periods. In general, the design criteria are not satisfactory in a very short-period range, for example less than 0.15 sec. Distribution of maximum response with periods is different from one earthquake motion to another, showing an irregular shape, although each hystersis model was designed on the basis of elastic response of individual earthquake motion. On the other hand, distribution of maximum response with periods is similar from one hysteresis model to another for a given earthquake motion, implying that maximum response amplitudes of different hysteresis models can be made comparable if hysteretic parameters of each model are properly adjusted.

Maximum response amplitudes of the six models are compared in Fig. 7.2 in two groups depending on the magnitude of hysteretic energy dissipation capacity per cycle. Hysteretic energy dissipation indices of these models are listed in Table 4.1. For the same value of unloading stiffness degradation parameter, the Takeda and Clough models give comparable maximum response amplitudes. For an unloading stiffness degradation parameter of 0.0, the regular bilinear model in general demands less ductility than the Clough and Takeda models having the same parameter value. The hysteretic energy dissipation index values of the Bilinear (α = 0.0) and Ramberg-Osgood models are larger than those of the Clough and Takeda models (α = 0.0) as listed in Table 4.1.

For an unloading stiffness degradation parameter of 0.5, the Takeda, Clough and Degrading Bilinear models developed comparable ductility factors. The Degrading Trilinear model also developed ductility factors similar in magnitude to those three

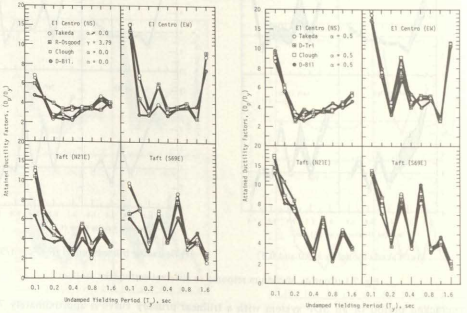

(a) Ramberg-Osgood, degrading bilinear, Clough and Takeda models (α = 0.0)

(b) Degrading bilinear, Clough, Takeda and Degrading trilinear Models (α = 0.5)

Fig. 7.2 Maximum response of different models

models at corresponding periods.

Therefore, maximum response amplitudes are not as sensitive to detail difference in hysteretic rules of these models, but rather are influenced by more basic characteristics of hysteresis loops, such as stiffness properties to define a primary curve and the fatness (hysteretic energy dissipating capacity) of a hysteresis loop.

Clough and Bilinear Takeda Models: The hysteresis rules of the two models are similar, having a bilinear primary curve and allowing the usage of unloading stiffness degradation parameter. The basic difference of the two models is that the Bilinear Takeda model has more hysteresis rules so that a response point during loading should move toward a peak response point of the immediately outer hysteresis loop.

Displacement response waveforms and hysteresis loops of the two models are compared in Fig. 7.3 The El Centro (NS) 1940 record is used for the response. The yielding period of the two models is 0.4 sec., and the unloading stiffness degradation parameter is 0.5. The response waveforms and hysteresis shapes of the two models are almost identical. The same observation was made for the two models using an unloading stiffness degradation parameter of 0.0. Some difference in displacement waveforms of the two models appeared after 8.0 sec. from the beginning of the earthquake motion, especially when the unloading stiffness degradation parameter is zero. When the

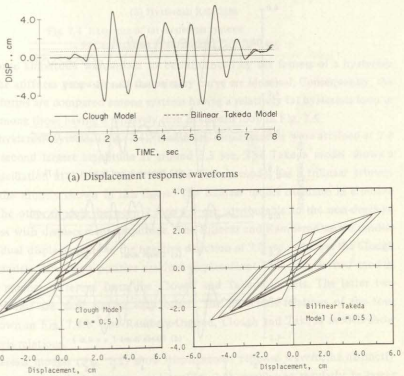

(a) Displacement response waveforms

(b) Hysteresis (Clough model)

(c) Hysteresis (Bilinear Takeda model)

Fig. 7.3 Response of Clough and bilinear Takeda models
– El Centro (NS) 1940 motion, T_y = 0.40 sec. –

parameter is large, say 0.5, the area of a hysteresis loop becomes smaller, and not much variation of inner hysteresis loops can be made possible within the limited area.

This is another example to demonstrate a less effect of detailed hysteretic rules on the response amplitude and response waveform, as long as the stiffness parameters to define a primary curve and basic hysteretic parameters are chosen to be the same.

Response Waveforms and Hysteresis Relations: Resistance response normally oscillates about its neutral axis, and its amplitude is limited by the yield resistance. On the other hand, displacement response does not necessarily oscillate about the neutral axis, but the residual displacement amplitude is easily shifted by the properties of a hysteretic model. Therefore, it is easy to study the effect of different hysteretic properties in a displacement response waveform.

The El Centro (NS) 1940 motion was used for response computation. Five hysteretic models were used for comparison; *i.e.*, (a) Degrading Bilinear model (α = 0.0 and 0.5), (b) Ramberg-Osgood model (γ = 3.79), (c) Clough model (α = 0.0 and 0.5), (d) Takeda model (α = 0.0 and 0.5), and (e) Degrading Trilinear model (F_c/F_y = 1/3). The yielding period of these models was arbitrarily chosen to be 0.4 sec., and the yield resistance level was taken to be 60 per cent of the standard model to allow a larger inelastic action.

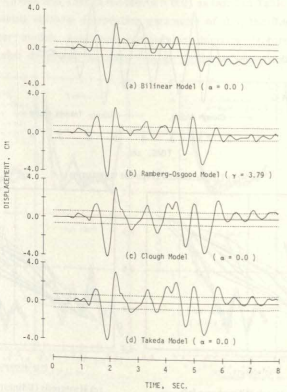

(a) Displacement Response Waveforms

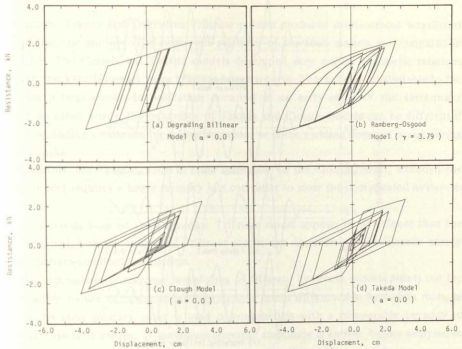

(b) Hysteresis Relations

Fig. 7.4 Response of fat-hysteresis systems
– El Centro (NS) 1940 motion, T_y = 0.40 sec. –

The response amplitude was shown to be influenced by the fatness of a hysteresis loop even if the stiffness properties of the primary curve are identical. Consequently, the response waveforms are compared among systems having a relatively fat hysteresis loop in *Fig. 7.4*, and among those having a relatively thin hysteresis loop in Fig. 7.5

In all fat-hysteresis systems (Fig. 7.4), maximum displacements were attained at 2.0 sec., and the second largest amplitude at around 5.3 sec. The Takeda model shows a short-period oscillation at 1.0 sec., since only the Takeda model has a trilinear primary curve among the models shown in this figure. The Bilinear model oscillates in a period shorter than the other models, between 2.5 to 4.5 sec. attributable to the non-degradation of stiffness with displacement amplitude. The Bilinear and Ramberg-Osgood models developed residual displacements in the negative direction at 7.0 sec., whereas the Clough and Takeda models developed positive residual displacement. The former two models behaved in a manner different from the Clough and Takeda models. The latter two response waveforms are very similar each other. The hysteresis relations of the four models are shown in Fig. 7.4.b. The Ramberg-Osgood, Clough and Takeda models show similar hysteresis relations.

Thin-hysteresis models (Fig. 7.5) show displacement reponse waveforms distinctly different from those of fat-hysteresis models (Fig. 7.4), oscillating regularly in larger amplitudes and in longer periods. The degrading Bilinear model exhibited a behaviour different from the other three models, especially in a waveform between 6.5 and 8.0 sec.

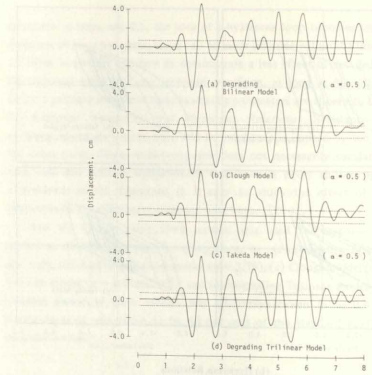

(a) Displacement Response Waveforms

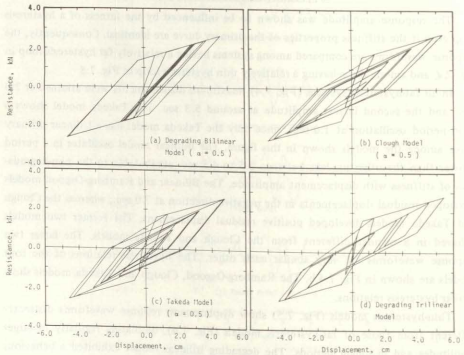

(b) Hysteresis relations

Fig. 7.5 Response of thin-hysteresis systems
– El Cento (NS) 1940 motion, T_y = 0.40 sec. –

The Clough, Takeda and Degrading Trilinear models produced displacement waveforms very similar one another. The hysteresis relations of the four models are compared in Fig. 7.5.b. The Clough and Takeda models developed very similar hysteretic relations although the Takeda model had a trilinear primary curve. This may be attributable to the fact that a large-amplitude oscillation occurred at an early stage of the earthquake motion. In other words, the behaviour of Takeda and Clough models can be different if a small oscillation continues for a long duration, or if the yielding does not occur during an earthquake.

Therefore, the Takeda model is more preferable to the Clough model, although the former model requires a larger memory in a computer to store the complicated hysteresis rules.

A hysteresis loop of the Degrading Trilinear model appears to be thinner than the Takeda model, but the Degrading Trilinear model can dissipate larger hysteretic energy during medium-amplitude oscillation.

The comparison of response waveforms of different hysteresis models points out the less sensitive nature of response waveforms to a minor difference in hysteresis rules, as long as the same primary curve is used in conjunction with a comparable capacity to dissipate hysteretic energy. If maximum response amplitude is known, before analysis, to be much larger than the yield displacement, the Clough model can produce a response waveform similar to that of the complicated Takeda model. However, if that premise is not guaranteed, it is more conservative to use a hysteresis model with a trilinear primary curve in the analysis of the reinforced concrete, recognizing the stiffness changes at cracking and yielding; *i.e.* the Takeda model.

8. Conclusions

The effect of dominantly flexural hysteretic models for the reinforced concrete on the earthquake response is studied by changing stiffness parameters. Hysteretic models used for study in this paper were (a) Degrading Bilinear model, (b) Ramberg-Osgood model, (c) Clough model, (d) Bilinear Takeda model, (e) Takeda model, and (f) Degrading Trilinear model.

Two types of viscous damping are used; *i.e.*, (a) constant mass-proportional damping, and (b) varying instantaneous stiffness-proportional damping. The mass-proportional damping is more effective in reducing maximum earthquake response amplitude, especially in a short-period system. The stiffness-proportional damping is less effective, especially if a system is capable of dissipating a large hysteretic energy.

Some stiffness properties of a primary curve have a strong influence on earthquake response amplitude. The level of yield resistance has a significant effect on maximum response amplitude of systems, especially in a short period range. The unloading stiffness degradation parameter, which controls the unloading stiffness and fatness of a hysteresis loop, is another important parameter. Post-yielding stiffness has a medium influence in a short-period system. Initial stiffness and cracking force level of a Takeda model have little

influence on the maximum amplitude if the attained ductility factor is 4.0 or higher. On the contrary, the cracking force level is an important parameter for a Degrading Trilinear model. A steep unloading stiffness tends to cause a large residual displacement. These stiffness and hysteretic properties need to be determined on the basis of material properties and geometry of the reinforced concrete.

If the stiffness properties of a primary curve and hysteretic energy dissipation capacity are properly selected, the maximum response amplitude does not change appreciably, nor does the response waveform from a hysteresis model to another. However, a complicated hysteresis model should not be penalized because the complicatedness simply requires a larger computer memory to store the program. Such a model does not require a longer computation time.

Acknowledgement

This reserch was initiated by the author in the Department of Civil Engineering, University of Toronto, supported by the National Research Council of Canada under Operational Grant A3739 (1976-81). Further computation was made in the Department of Architecture, University of Tokyo, supported by the National University Research Fund. These research supports are gratefully acknowledged.

References

1. Amin, M. and A.H.-S.Ang, "A Nonstationary Model for Strong Motion Earthquakes", Structural Research Series No.306, University of Illinois, Urbana, 1966.
2. Clough, R.W. and S.B. Johnston, "Effect of Stiffness Degradation on Earthquake Ductility Requirements", Proceedings, Second Japan National Conference on Earthquake Engineering, 1966, pp.227-32.
3. Fukada, Y., "Study on the Restoring Force Characteristics of Reinforced Concrete Buildings (In Japanese)", Proceedings, Kanto District Symposium, Architectural Institute of Japan, No.40, 1969, pp.121-4.
4. Gulkan, P. and M.A. Sozen, "Inelastic Response of Reinforced Concrete Structures to Earthquake Motion", Journal, ACI, No.12, Vol. 71, 1974, pp.604–10.
5. Hisada, T., K. Nakagawa and M. Izumi, "Earthquake Response of Structures Having Various Restoring Force Characteristics", Proceedings, Japan National Conference on Earthquake Engineering, 1962, pp.63–8.
6. Jennings, P.C., "Response of Simple Yielding Structures to Earthquake Excitation", Ph.D. Thesis, California Institute of Technology, Pasadena, 1963.
7. Mahin, S.A. and V.V. Bertero, "Rate of Loading Effect on Uncracked and Repaired Reinforced Concrete Members", EERC 73-6, Earthquake Engineering Research Center, University of California, Berkeley, 1972.
8. Mahin, S.A. and V.V. Bertero, "Nonlinear Seismic Response of a Coupled Wall System", Journal, Structural Division, ASCE, Vol.102, No.ST9, 1976, pp.1759-80.
9. Newmark, N.M., "A Method of Computation for Structural Dynamics", Journal, Engineering Mechanics Division, ASCE, Vol.85, No.EM3, 1959, pp.67-94.
10. Nielsen, N.N. and F.A. Imbeault, "Validity of Various Hysteretic Systems", Proceedings, Third Japan National Conference on Earthquake Engineering, 1971, pp.707–14.
11. Otani, S. and M.A. Sozen, "Behavior of Multistory Reinforced Concrete Frames During Earthquakes", Structural Research Series No. 392, University of Illinois, Urbana, 1972.
12. Otani, S., "Nonlinear Dynamic Analysis of Reinforced Concrete Building Structures", Canadian Journal of Civil Engineering, Vol. 7, No. 2, 1980, pp.333–44.
13. Otani, S., "Effect of Hysteretic Characteristics on Earthquake Response (In Japanese)", Proceedings, 26th Symposium on Structural Engineering, Japan, 1980, pp.29–40.
14. Otani, S. and V.W.-T. Cheung, "Behaviour of Reinforced Concrete Columns Under Biaxial Lateral Load Reversals – (II) Test Without Axial Load", Publication 81-02, Department of Civil Engineering, University of Toronto, 1981.
15. Ramberg, W. and W.R. Osgood, "Description of Stress-Strain Curves by Three Parameters", National Advisory Committee on Aeronautics, Technical Note 902, 1943.
16. Takeda, T., M.A. Sozen, and N.N. Nielsen, "Reinforced Concrete Response to Simulated Earthquakes", Journal, Structural Division, ASCE, Vol. 96, No. ST.12, 1970, pp.2557–73.
17. Tani, S., S. Nomura, T. Nagasaka and A. Hiramatsu, "Restoring Force Characteristics of Reinforced Concrete Seismic Elements-III Influence of Restoring Force Characteristics on Dynamic Response of Structure (In Japanese)", Transaction, AIJ, No. 228, 1975, pp.39–48.
18. Umemura, H. editor, *Dynamic Design for Earthquakes of Reinforced Concrete Buildings* (In Japanese), Giho-do Publishing Co., Japan, 1973.
19. Veletsos, A.S. and N.M. Newmark, "Effect of Inelastic Behavior on the Response of Simple Systems to Earthquake Motions", Proceedings, Second World Conference on Earthquake Engineering, 1960, Vol. II, pp.895–912.